Diffusion in Confined Geometries

P. Sekhar Burada,[a] Peter Hänggi,*[a] Fabio Marchesoni,[b] Gerhard Schmid,[a] and Peter Talkner[a]

Diffusive transport of particles or, more generally, small objects, is a ubiquitous feature of physical and chemical reaction systems. In configurations containing confining walls or constrictions, transport is controlled both by the fluctuation statistics of the jittering objects and the phase space available to their dynamics. Consequently, the study of transport at the macro- and nanoscales must address both Brownian motion and entropic effects. Herein we report on recent advances in the theoretical and numerical investigation of stochastic transport occurring either in microsized geometries of varying cross sections or in narrow channels wherein the diffusing particles are hindered from passing each other (single-file diffusion). For particles undergoing biased diffusion in static suspension media enclosed by confining geometries, transport exhibits intriguing features such as 1) a decrease in nonlinear mobility with increasing temperature or also 2) a broad excess peak of the effective diffusion above the free diffusion limit. These paradoxical aspects can be understood in terms of entropic contributions resulting from the restricted dynamics in phase space. If, in addition, the suspension medium is subjected to external, time-dependent forcing, rectification or segregation of the diffusing Brownian particles becomes possible. Likewise, the diffusion in very narrow, spatially modulated channels is modified via contact particle–particle interactions, which induce anomalous sub-diffusion. The effective sub-diffusion constant for a driven single file also develops a resonance-like structure as a function of the confining coupling constant.

1. Introduction

Effective control of transport in artificial micro- and nanostructures requires a deep understanding of the diffusive mechanisms involving small objects and, in this regard, an operative measure to gauge the role of fluctuations. Such situations are typically encountered when studying the transport of particles in biological cells[1] and in zeolites,[2] catalytic reactions occurring on templates or in porous media,[3] chromatography or, more generally, separation techniques of size-dispersed particles on micro- or even nanoscales.[4] In many respects studying these transport phenomena is equivalent to studying geometrically constrained Brownian dynamics.[5–7] The fact that the diffusion equation is closely related to the time evolution of the probability density $P(\vec{x},t)$ to find a jittering particle at a location $\vec{x}$ at time t dates back to Einstein's pioneering work on the molecular–kinetic description of suspended particles.[8]

Herein we focus on the problem of the diffusion of small particles in confined geometries. Restricting the volume of the phase space available to the diffusing particles by means of confining boundaries or obstacles causes remarkable entropic effects.[9] The driven transport of charged particles across bottlenecks, such as ion transport through artificial nanopores or artificial ion pumps[10–15] or in biological channels[16–20] represents an ubiquitous situation, where diffusion is determined by entropic barriers. Similarly, the operation of artificial Brownian motors,[21–23] molecular motors[24] and molecular machines[25] also results from the interplay of diffusion and binding action by energetic or, more relevant in the present context, entropic barriers.[26] The efficiency of such nanodevices crucially depends on the fluctuation characteristics of the relevant degrees of freedom.[27] In addition, the interplay of diffusion over entropic barriers and unbiased time-periodic drives is responsible for certain perplexing transport effects, like the recent observation of entropic diffusion-controlled absolute negative mobility.[28]

Although we restricted ourselves to small particles, we remind the reader that entropic forces surely affect the dynamics of extended chains diffusing in a periodic two- (2D) or three-dimensional (3D) medium. A well-established example is represented by the phonon damping of propagating solitons.[29] Another example of great interest for its potential applications in nanotechnology is the translocation of a long polymer molecule through a pore with opening size comparable to the polymer gyration radius. In this case, entropic effects were first predicted to describe theoretically the conformational changes the chain undergoes to move past a conduit constriction[30] and, then, experimentally observed both in biological[31] and artificial channels.[32]

Another instance of constrained Brownian dynamics that rests, indeed, within the scope of our Minireview, is known as single-file diffusion. The motion of an assembly of small particles in a narrow channel can be so tightly restricted in the transverse directions that the particles arrange themselves one

[a] *Dr. P. S. Burada, Prof. Dr. Dr. h.c. mult. P. Hänggi, Dr. G. Schmid, Prof. Dr. P. Talkner*
Institut für Physik
Universität Augsburg, Universitätsstr. 1
86135 Augsburg (Germany)
Fax: (+49) 821 598 3222
E-mail: hanggi@physik.uni-augsburg.de

[b] *Prof. Dr. F. Marchesoni*
Dipartimento di Fisica
Università di Camerino, Via Madonna delle Carceri 9
62032 Camerino (Italy)

by one into a single file. The longitudinal motion of each particle is thus hindered by the presence of its neighbors, which act as impenetrable movable obstacles. As a consequence, interparticle interactions in one dimension can suppress Brownian diffusion and lead to the emergence of a new subdiffusive dynamics.[33]

Herein, we discuss the geometry of the channels relevant to our review and set up the mathematical formalism needed to model the diffusion of a Brownian particle immersed in a confined suspension fluid. We introduce some exact results for the mobility and the diffusion coefficient of a driven Brownian particle in a 1D periodic potential and we compute explicitly the entropic effects on particle transport in a static fluid filling a periodically modulated channel. We also address particle transport in a suspension fluid flowing along the channel subject to stationary pumping. We review numerical and analytical results for the diffusion of a single file along a periodically corrugated channel both in the presence and in the absence of an external drive.

2. Channel Models

We consider the diffusive dynamics of spherical particles in 2D or 3D pores, or channels, which extend in the x direction and possess a periodically varying cross section. These channels are supposed to be symmetric with respect to a 2D reflection on the channel axis (like those sketched in Figure 1), or to any rotation about the channel axis in 3D. The channels are assumed to be delimited by smooth, rigid walls. The half-width of the channel is described by the well-behaved boundary function $w(x)$. The channel walls confine the particles inside the channel, but do not exchange energy with them otherwise. In particular, we do not consider the possibility of adsorption of particles on the walls. Since we disregard any rotatory motion of the particles about their centers of mass, we need not specify particle–wall contact forces. Moreover, the radius of the particles is supposed to be smaller than the minima of $w(x)$ [channel bottlenecks], so that they are not restricted to stay within a confined region of the channel, but rather may diffuse everywhere along the channel.

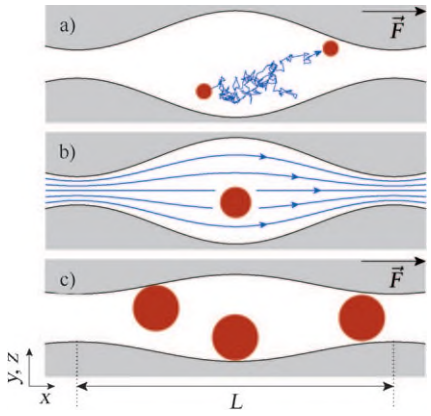

Figure 1. Brownian particles in a narrow cylindrical channel directed along the x axis and with a periodically modulated boundary $w(x)$ [longitudinal section]. a) Pointlike particle suspended in a static fluid and subjected to a constant driving force F (Section 4); b) Single spherical particle dragged along by a laminar flow (Section 5); c) Single-file diffusion of impenetrable driven particles (Section 6.2).

2.1. Diffusion Equations

The motion of particles that are immersed in a fluid medium is influenced by various types of forces. Herein, we restrict ourselves to the discussion of small-radius (almost pointlike) particles, whose presence do not significantly modify the free motion of the fluid around them (laminar flow regime). The systematic impact of the fluid on the motion of particles at position $\vec{x} \equiv (x,y,z)$ is given in Equation (1) by the Stokes force:[34]

$$\vec{F}_{\text{Stokes}} = -\gamma\left[\dot{\vec{x}} - \vec{v}(\vec{x},t)\right] \tag{1}$$

where $\vec{v}(\vec{x},t)$ is the instantaneous velocity of the fluid in absence of the particle, $\dot{\vec{x}}$ is the instantaneous particle velocity, and the friction constant is given by Equation (2):

$$\gamma = 6\pi\eta R \tag{2}$$

The friction constant is determined by the shear viscosity η of the fluid, and the radius R of the particle. At the same time, the fluid also exerts a random thermal force $\vec{F}_{\text{th}}$ on the particle. In the following, we only deal the case of fluids at a homogeneous temperature T and velocity fields that are almost constant on the particle scale R. As a consequence, to insure thermalization at temperature T it suffices to set the thermal force in Equation (3) to:

$$\vec{F}_{\text{th}}(t) = \sqrt{2\gamma k_{\text{B}} T}\,\vec{\xi}(t), \tag{3}$$

where k_{B} denotes the Boltzmann constant and $\vec{\xi}(t)$ is a standard 3D Gaussian noise with $\langle\vec{\xi}(t)\rangle = 0$ and $\langle\xi_{\text{i}}(t)\xi_{\text{j}}(t')\rangle = \delta_{\text{ij}}\delta(t-t')$for $i,j = x,y,z$. Other forces acting on the particles, like hydrodynamic interactions among different particles and between single particles and the wall, are neglected.[35,36] This simplification, in particular, requires a sufficiently low particle density.

Finally, an external force $\vec{F}_{\text{ext}}$ may act on the particles describing for example, the gravity force, or in the case of charged particles, an electrostatic force. We further restrict our discussion to constant longitudinal external forces pointing in the direction of the symmetry axis of the channel. The dynamics of the center of mass $\vec{x}(t)$ of a single particle of mass m is then governed by Newton's equation of motion, Equation (4):

$$m\ddot{\vec{x}} = \vec{F}_{\text{ext}} - \gamma\left[\dot{\vec{x}} - \vec{v}(\vec{x},t)\right] + \sqrt{2\gamma k_{\text{B}} T}\,\vec{\xi}(t) \tag{4}$$

where we explicitly allow for a possible time-dependence of the fluid velocity field. For microparticles moving with typical velocities of the order of $1\,\text{cm}\,\text{s}^{-1}$, the inertial term $m\ddot{\vec{x}}(t)$ in Equation (4) is negligibly small compared to the environmental

forces;[37] therefore, provided that the fluid velocity does not change too fast, that is, for spectral frequencies less than a few 100 Hz, one can safely set $m=0$ (overdamped limit or Smoluchowski approximation). Under these conditions, Equation (4) can be simplified to Equation (5):

$$\dot{\vec{x}} = \vec{v}(\vec{x},t) + \frac{1}{\gamma}\vec{F}_{\text{ext}} + \sqrt{\frac{2k_{\text{B}}T}{\gamma}}\vec{\xi}(t) \tag{5}$$

This Langevin equation is equivalent to the Fokker–Planck equation[38] for the probability density $P(\vec{x},t)$ of a particle to be found at the position $\vec{x}$ at time t, given by Equation (6):

$$\frac{\partial P(\vec{x},t)}{\partial t} = -\vec{\nabla}\cdot\vec{J}(\vec{x},t) \tag{6}$$

Here $\vec{J}(\vec{x},t)$ denotes the corresponding probability current density of Equation (7):

$$\vec{J}(\vec{x},t) = -\left[\vec{v}(\vec{x},t) + \frac{\vec{F}_{\text{ext}}}{\gamma}\right]P(\vec{x},t) + \frac{k_{\text{B}}T}{\gamma}\vec{\nabla}P(\vec{x},t) \tag{7}$$

These equations have to be supplemented by appropriate boundary conditions, discussed next.

2.2. Boundary Conditions

A channel is typically characterized by two boundary regions. A transverse boundary naturally results from the presence of the walls, whereas a longitudinal boundary is required to account for the channel length.

The probability flux normal to the boundary in the presence of a rigid hard wall must vanish. Thus, to prevent pointlike particles from leaving the channel or being adsorbed at the walls, we must impose Equation (8):

$$\vec{n}(\vec{x})\cdot\vec{J}(\vec{x},t) = 0 \quad \vec{x}\in \text{wall} \tag{8}$$

where $\vec{n}(\vec{x})$ denotes the unit vector normal to the wall at point $\vec{x}$. Note, however, that the center of mass of a spherical particle of finite radius R may approach the wall only up to a distance R, so that for finitely sized particles the boundary conditions of Equation (8) applies on an appropriate inner surface parallel to the channel walls.[39]

Various kinds of boundary conditions exist that regulate the inward and outward probability flows at the ends of a channel.[34] If the channel connects large, well-mixed particle reservoirs, then constant probability densities $P_{\text{L,R}}$ may be assigned at the channel ends. This leads to Dirichlet boundary conditions given by Equation (9):

$$P(x_{\text{L}},y,z) = P_{\text{L}}, \quad P(x_{\text{R}},y,z) = P_{\text{R}} \tag{9}$$

where x_{L} and x_{R} denote the left and right endpoints of the channel, respectively. A more detailed description of the particle flow into and out of a channel is achieved by relating flux and probability densities at $x=x_{\text{R,L}}$, as in Equation (10):[40]

$$\begin{aligned} J_x(x_{\text{L}},y,z,t) &= -\kappa_{\text{L}}P(x_{\text{L}},y,z,t) \\ J_x(x_{\text{R}},y,z,t) &= \kappa_{\text{R}}P(x_{\text{R}},y,z,t) \end{aligned} \tag{10}$$

Positive (negative) constants $\kappa_{\text{L,R}}$ correspond to partially absorbing (emitting) boundaries. As special cases, reflecting and absorbing boundaries correspond to $\kappa_{\text{R,L}}=0$ and $\kappa_{\text{R,L}}=\infty$, respectively.

Finally, for an infinitely long channel the periodic boundary conditions given by Equation (11):

$$P(x,y,z,t) = P(x+L,y,z,t) \tag{11}$$

are more appropriate.[38] In the case of velocity fields which are constant with respect to time or vary periodically in time, these boundary conditions allow for stationary-flux-carrying solutions.[21–23]

3. Exact Results for 1D Systems

In order to set the stage, we first consider the ideal case where the diffusion of a particle in a periodically corrugated channel can be simulated by diffusion on an energetic landscape represented, for simplicity, by a 1D periodic potential $V(x)$ with period L, namely $V(x+L)=V(x)$. Such a system is often employed to model, for instance, nanotube[41] and zeolite diffusion.[2] Let us consider a Brownian particle with mass m, coordinate x, and friction coefficient γ, subject to a static external force F and a thermal noise $F_{\text{th}}(t)$. In the notation of Section 2.1, we set $F_{\text{ext}}=-V'(x)+F$ and $v(x,t)\equiv 0$.

The corresponding stochastic dynamics is described by the Langevin equation [Eq. (12)]:

$$m\ddot{x} = -V'(x) - \gamma\dot{x} + F + \sqrt{2\gamma k_{\text{B}}T}\xi(t) \tag{12}$$

where $\xi(t)$ is the standard Gaussian noise also defined in Section 2.1. Moreover, herein the potential $V(x)$ can be taken as symmetric under reflection, $V(x)=V(-x)$.

In extremely small systems, particle fluctuations are often described to a good approximation by the *overdamped* limit of Equation (12), that is, by the massless Langevin equation given by Equation (13):

$$\gamma\dot{x} = -V'(x) + F + \sqrt{2\gamma k_{\text{B}}T}\xi(t) \tag{13}$$

where the inertia term $m\ddot{x}$ has been dropped altogether (Smoluchowski approximation).

An overdamped particle is trapped most of the time at a local minimum of the tilted potential as long as $F \le F_3$, F_3 denoting the depinning threshold $F_3 = \max\{V'(x)\}$. Drift occurs by rare noise-induced hopping events between adjacent minima. There are no such minima for $F > F_3$ and the particle runs in the F direction with average speed approaching the constant F/γ. This behavior is described quantitatively by the mobility formula of Equation (14):

$$\mu(F) \equiv \frac{\langle \dot{x} \rangle}{F} \tag{14}$$

where $\langle \dot{x} \rangle$ is given by Equation (15):

$$\langle \dot{x} \rangle \equiv \lim_{t \to \infty} \frac{\langle x(t) \rangle}{t} = \frac{L}{\langle t(L,F) \rangle} \tag{15}$$

Here and in the following, $\langle t^n(L,F) \rangle$ denotes the nth moment of the first passage time $t(L,F)$[42,43] of the particle crossing a unit cell of the potential energy function in the F direction.

As the particle drifts subjected to the external force F, the random hops cause a spatial dispersion of the particle around its average position $\langle x(t) \rangle$. The corresponding *normal* diffusion coefficient, given by Equation (16):

$$D(F) \equiv \lim_{t \to \infty} \frac{\langle x(t)^2 \rangle - \langle x(t) \rangle^2}{2t} \tag{16}$$

can be computed analytically by regarding the hopping events in the overdamped regime as manifestations of a renewal process, as in Equation (17):[44]

$$D(F) = L^2 \frac{\langle t^2(L,F) \rangle - \langle t(L,F) \rangle^2}{2\langle t(L,F) \rangle^3} \tag{17}$$

Simple algebraic manipulations lead to explicit expressions for the nonlinear mobility, Equation (18):[38,45,46,43]

$$\mu(F) = \frac{D_0 L}{F} \frac{1 - e^{-LF/k_B T}}{\int_0^L I_+(x)dx} \tag{18}$$

and for the diffusion coefficient, Equation (19):[44]

$$\frac{D(F)}{D_0} = L^2 \int_0^L I_+^2(x) I_-(x) dx \cdot \left[\int_0^L I_+(x) dx \right]^{-3} \tag{19}$$

Here, $I_\pm(x) = \int_0^L \exp[(\pm V(x) \mp V(x \mp y) - yF/k_B T]dy$ and $D_0 = k_B T/\gamma$ denotes Einstein's coefficient for a freely diffusing Brownian particle.

For $F \to 0$ Equations (18) and (19) reproduce the zero-bias identity $D(0)/D_0 = \gamma\mu(0)$ with $\mu(0) = L^2/\left[\gamma \int_0^L I_+(x)dx\right]$.[38,47] Notably, as F approaches the depinning threshold F_3 the mobility curve [Eq. (18)] jumps from zero (locked state) up to close to $1/\gamma$ (running state). Correspondingly, the diffusion coefficient [Eq. (19)] develops a diffusion excess peak, that is, with $D > D_0$, consistently with numerical observations in ref. [48]. Both the mobility step and the D peak get sharper and sharper as T is lowered.[44] The same conclusions apply in the presence of inertia (i.e. for particles of finite mass m)[48,49] as well, with the difference that the relevant depinning threshold shifts towards lower values (proportionally to γ as $\gamma \to 0$.[38])

Finally, we emphasize that the above formulas for the nonlinear mobility and the effective diffusion coefficient retain their analytic structure even when generalized to anomalous (sub)diffusion on a 1D substrate, by merely substituting the normal diffusion constant D_0 by the fractional diffusion constant occurring in the corresponding fractional diffusion equation.[50]

4. Particle Diffusion in a Static Fluid

In the limiting case of pointlike particles with zero interaction radius diffusing in constrained 2D or 3D geometries, elastic contact particle–particle interactions can be neglected. As long as hydrodynamically mediated interactions can also be neglected,[35,36] the confining action of the channel walls is modeled by the perfectly reflecting boundary conditions of Equation (8).

In the presence of a constant external force pointing in the channel direction, an overdamped Brownian particle suspended in a static medium is described by the Langevin equation [Eq. (5)], or by the corresponding Fokker–Planck equation [Eq. (6)], both with zero velocity field $\vec{v}(\vec{x}, t) \equiv 0$. For a general choice of the periodic boundary $w(x)$, no exact analytical solutions to the Fokker–Planck Equation (6) with the boundary conditions of Equation (8) exist. However, approximate solutions can be obtained by reducing the problem of free Brownian diffusion in a 2D or 3D channel to that of Brownian diffusion on an effectively 1D periodic potential. Under such a scheme, narrow channel constrictions, corresponding to geometric hindrances in the fully dimensional problem, are modeled as entropic 1D barriers.

In the absence of external forces, that is, for $\vec{F}_{ext} = 0$, particle dynamics in confined structures [see Figure 1 (a)] can be approximately described by the Fick–Jacobs kinetic equation with a spatially dependent diffusion coefficient, as given by Equation (20):[51–54]

$$\frac{\partial P(x,t)}{\partial t} = \frac{\partial}{\partial x} \left[D(x)\sigma(x) \frac{\partial}{\partial x} \frac{P}{\sigma(x)} \right] \tag{20}$$

with $\sigma(x)$ denoting the dimensionless channel cross-section $2w(x)/L$ in 2D and $\pi w^2(x)/L^2$ in 3D. Equation (20) is obtained[52] from the full Fokker–Planck equation[Eq. (6)] for small-amplitude boundary modulations $w(x)$, on assuming a transversally uniform density $P(\vec{x}, t)$ and integrating out the transverse coordinates [for example, for a 2D channel $P(x,t) = \int_{-w(x)}^{w(x)} dy P(x,y,t)$]. At variance with the original Fick–Jacobs equation,[51] introducing an x-dependent diffusion coefficient considerably improves the accuracy of the kinetic equation [Eq. (20)], thus extending its validity to larger $w(x)$ amplitudes.[52–54] Here, Equation (21):

$$D(x) = \frac{D_0}{[1 + w'(x)^2]^\alpha} \tag{21}$$

with $\alpha = 1/3$ in 2D and $\alpha = 1/2$ in 3D, is determined best to account for wall curvature effects.[53,55]

In the presence of weak longitudinal drives F, the Fick–Jacobs equation [Eq. (20)] can be extended further to Equation (22):[53,55,56]

$$\frac{\partial P}{\partial t} = \frac{\partial}{\partial x} D(x) \left[\frac{\partial P}{\partial x} + \frac{A'(x)}{k_B T} P \right] \tag{22}$$

where the free energy $A(x) = E(x) - TS(x)$ is made up of an energy, $E(x) = -Fx$, and an entropic term, $S(x) = k_B \ln \sigma(x)$. For a periodic channel, $A(x)$ assumes the form of a tilted periodic potential. Moreover, for a straight channel, $w'(x) = 0$, the entropic contributions vanish altogether and the particle is only subject to the external drive. Of course, for $F = 0$ the free energy is purely entropic and Equation (22) reduces to the Fick–Jacobs equation [Eq. (20)]. An alternative reduction scheme based on macrotransport theory has been proposed recently in ref. [57].

Key quantifiers of the reduced 1D kinetics of Equation (22) are the average *particle current* or, equivalently, the nonlinear mobility [Eq. (14)], and the effective diffusion coefficient [Eq. (17)] defined in Section 3. On generalizing the derivation of Equations (18) and (19) to account for the x-dependence of $D(x)$, one obtains,[56] respectively, Equations (23)

$$\gamma\mu(f) = \frac{1 - e^{-f}}{f \int_0^L \frac{dx}{L} I(x)} \tag{23}$$

and (24)

$$\frac{D_{\text{eff}}}{D_0} = \int_0^L \frac{dx}{L} \int_{x-L}^{x} \frac{dz}{L} \frac{D(z)}{D(x)} \frac{e^{A(x)/k_B T}}{e^{A(z)/k_B T}} [I(z)]^2 \cdot \left[\int_0^L \frac{dx}{L} I(x) \right]^{-3} \tag{24}$$

where $I(x)$ is given by Equation (25):

$$I(x) = \frac{e^{A(x)/k_B T}}{D(x)/D_0} \int_{x-L}^{x} \frac{dy}{L} e^{-A(y)/k_B T} \tag{25}$$

and the dimensionless force f is defined as the ratio of the work done by F to drag the particle a distance L, to the thermal energy $k_B T$, that is, Equation (26):

$$f = \frac{FL}{k_B T} \tag{26}$$

Here, we stress an important difference to the energetic 1D model of Section 3. For a particle moving in a 1D periodic potential $V(x)$, the barriers ΔV separating the potential wells provide an additional energy scale besides FL and $k_B T$, so that the particle dynamics is governed by at least two dimensionless energy parameters, say, $\Delta V/k_B T$ and $FL/k_B T$.[38] In contrast, Brownian transport in a periodically corrugated 2D or 3D channel is solely determined by the dimensionless force f.[56] This can be proven by rescaling the problem units as follows. We measure all lengths in units of the period L and time in units of $\tau = L^2/D_0$, that is, twice the time the particle takes to diffuse a distance L at temperature T. In these new dimensionless variables the Langevin Equation [Eq. (5)] for a Brownian particle in a static medium reduces to Equation (27):

$$\dot{\vec{x}}(t) = \vec{f} + \vec{\xi}(t) \tag{27}$$

with no tunable constants.[58] As a consequence, the ensuing Brownian dynamics is controlled only by the parameter f and, of course, by the additional lengths that possibly enter the boundary function $w(x)$.

The f-dependence of the average particle current [Eq. (23)] and the effective diffusion [Eq. (24)] were compared with the results obtained by numerical integration of the 2D Langevin equation [Eq. (5)] (for details see ref. [55]). For simplicity, the channel walls were assumed to have the sinusoidal profile given by Equation (28):

$$w(x) = a[\sin(2\pi x/L) + \kappa], \tag{28}$$

with $a > 0$ and $\kappa > 1$. Here, $a(\kappa \pm 1)$ are, respectively, the maximum and the minimum channel half-width. Moreover, a/L controls the slope of the boundary function $w(x)$, which in turn determines the modulation amplitude of the diffusion coefficient $D(x)$ in Equation (21). The mobility μ, Equation (14), and the corresponding effective diffusion coefficient D, Equation (16), were computed by ensemble averaging 3×10^4 simulated trajectories.

The most significant results are displayed in Figures 2 and 3. At variance with the purely energetic 1D models of Section 3, the nonlinear mobility decreases upon increasing the strength of thermal noise. Moreover, an enhancement of the effective diffusion coefficient, with maximum exceeding the free diffusion constant D_0, was also observed.[56,58]

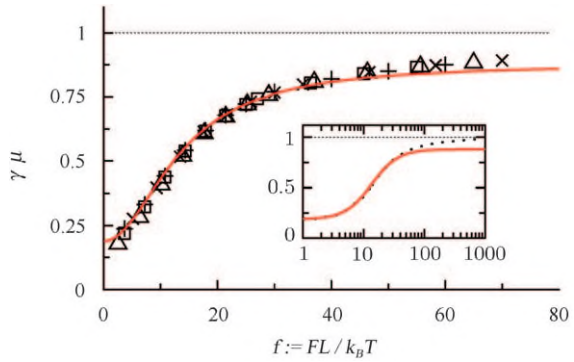

Figure 2. Nonlinear mobility μ vs driving force in dimensionless units, $f = FL/k_B T$, for a 2D channel at different temperatures $k_B T = 0.01$ (×), 0.1 (+), 0.2 (□), and 0.4 (△). After rescaling, all data sets collapse onto one curve which at low f closely compares with the analytic approximation [Eq. (23), ——]. Other simulation parameters are $L = 1$, $\gamma = 1$, and $w(x) = [\sin(2\pi x) + 1.02]/2\pi$. The inset shows the deviation of the analytic approximation [Eq. (23), ——] from the numerical results (•••••) for large f. Note that the numerical curve approaches the correct asymptotic limit $\gamma\mu = 1$.

At low values of the control parameter f the analytical approximations given by Equations (23) and (24) perfectly match the corresponding numerical curves, whereas deviations occur at high f. Most remarkably, contrary to the simulation output, the analytical curves for D_{eff}/D_0 and $\gamma\mu$ fail to attain the correct asymptotic limit 1 for $f \to \infty$ (see insets in Figures 2 and 3). This occurs because the assumption of transversally uniform density distribution, introduced in the Fick–Jacobs formalism

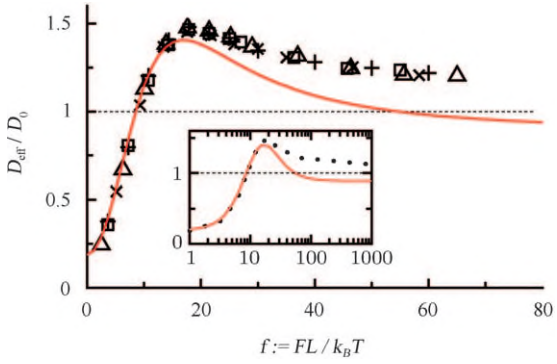

Figure 3. Effective diffusion coefficient D_{eff} vs f for the same simulation parameters as in Figure 2 [$k_BT = 0.01$ (×), 0.1 (+), 0.2 (□), and 0.4 (△)]. Here, too, the rescaled data collapse onto one curve, which asymptotically approaches the correct limit $D_{eff}/D_0 = 1$ (inset). The analytic approximation [Eq. (24), ——] fits the raising branch of the numerical data sets well.

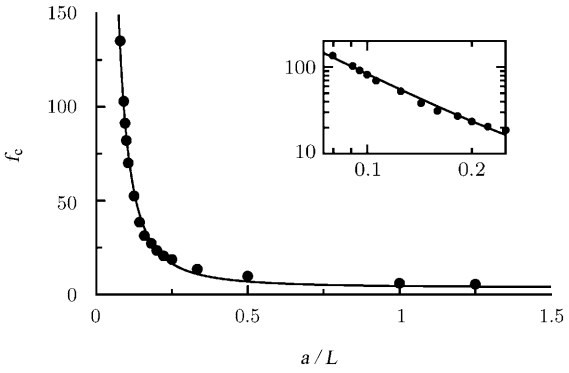

Figure 4. Critical force f_c vs boundary modulation amplitude a for the 2D channel of Figure 2. Other simulation parameters are $L = 1$, $\gamma = 1$, and $k_BT = 0.1$. The numerical values of f_c (●) were obtained by requiring that deviations of the Fick–Jacobs approximation from the simulation results remain smaller than ~1%. (——) is the fitting law $f_c = c_1(L/a)^2 + c_2$ with $c_1 = 0.792$ and $c_2 = 3.524$. The apparent discrepancy with Equation (32) results from the above-mentioned numerical accuracy criterion and is expected to vanish for higher accuracy. Inset: Same data sets on a logarithmic scale.

to eliminate the transverse coordinates, is no more tenable in the presence of strong drives.

The agreement between theory and numerics improves for smooth modulations of the channel walls, that is, for small boundary slopes $|w'(x)|$, which can be achieved, among others, for appropriately small a.[55,58] A phenomenological criterion to asses the validity of the stationary state solutions of the Fick–Jacobs Equation (22) can be formulated by comparing the different characteristic time scales of the problem, namely the diffusion times in the transverse direction, given by Equation (29):

$$\tau_{\perp}^{(d)} = (2a^2/D_0)(1+\kappa)^2 \tag{29}$$

and in the longitudinal direction [Eq. (30)]:

$$\tau_{\parallel}^{(d)} = L^2/2D_0 \tag{30}$$

and also the drift time the applied force F takes to drag the particle one channel unit length L across, given by Equation (31):

$$\tau_{\parallel}^{(f)} = \gamma L/F \tag{31}$$

Uniform probability distribution in the transverse direction sets in only if the transverse diffusion motion of the particle is sufficiently fast relative to both the diffusive and the drift longitudinal motions, which implies $\tau_{\perp}^{(d)} \ll \min\left\{\tau_{\parallel}^{(d)}, \tau_{\parallel}^{(f)}\right\}$. For large drives it suffices to require that $\tau_{\perp}^{(d)} \ll \tau_{\parallel}^{(f)}$, which leads to Equation (32):[58]

$$f \le f_c \equiv \frac{1}{2(1+\kappa)^2}\left(\frac{L}{a}\right)^2 \tag{32}$$

The critical force parameter f_c, above which the Fick–Jacobs description is expected to fail, depends on the remaining free parameters of the problem. For the boundary function, Equation (28), f_c is a function of a/L, alone, as illustrated in Figure 4. For $a \gg L$ the Fick–Jacobs approximation already becomes untenable for relatively small forces f, whereas for $a \ll L$ its validity extends to significantly larger drives.

5. Particle Diffusion in Moving Fluids

Let us assume now that a small, spherical particle is swept along in the time-periodic velocity field $\vec{v}(\vec{x}, t)$ of a moving, incompressible fluid (see Figure 1 b), rather than by a constant force, $\vec{F}_{ext}$, as in Section 4. For $\vec{F}_{ext} = 0$, its dynamics is then described by the Langevin equation, in the overdamped limit of Equation (33):

$$\dot{\vec{x}}(t) = \vec{v}[\vec{x}(t), t] + \sqrt{\frac{2k_BT}{\gamma}}\vec{\xi}(t) \tag{33}$$

where the fluid velocity field $\vec{v}(\vec{x}, t)$ is to be determined.

To this end, we first write the Stokes equations for stationary incompressible flow in the limit of vanishing Reynolds numbers (the convective acceleration terms in the Navier–Stokes equations can safely be neglected). One obtains the "creeping flow equation", Equation (34):[34]

$$\eta\Delta\vec{v}(\vec{x}) = \vec{\nabla}p(\vec{x}) \tag{34}$$

where $p(\vec{x})$ is the pressure field responsible for the stationary laminar flow of the fluid and η is the shear viscosity. On introducing the scalar field $\Psi(x,r)$, with (r,ϕ) being the polar coordinates in the transverse plane (y,z), $\vec{v}(\vec{x})$ can be rewritten as Equation (35):[34]

$$\vec{v}(x,r) = \vec{\nabla} \times [\Psi(x,r)\vec{e}/r] \tag{35}$$

where $\vec{e}$ is the unit ϕ vector. On substituting Equation (35) into the creeping flow equation [Eq. (34)], one obtains Equation (36), a linear homogeneous fourth-order differential equa-

tion:[34,59]

$$\left(r\frac{\partial}{\partial r}\frac{1}{r}\frac{\partial}{\partial r}+\frac{\partial^2}{\partial x^2}\right)^2\Psi(x,r)=0 \tag{36}$$

with boundary conditions given by Equations (37)–(40):

$$\Psi|_{r=0}=c \tag{37}$$

$$\frac{\partial}{\partial r}\Psi|_{r=0}=\frac{\partial^3}{\partial r^3}\Psi|_{r=0}=0 \tag{38}$$

$$\vec{\nabla}\Psi[x,r=w(x)]=0 \tag{39}$$

$$\Psi(x+L,r)=\Psi(x,r) \tag{40}$$

where c is an arbitrary constant. Solutions to Equation (36) determine the velocity field $\vec{v}(\vec{x})$ up to a multiplicative factor, which, in turn, can be established by imposing an additional condition, for example, for the pressure drop across a channel unit, that is, Equation (41):[59]

$$p(x,r)-p(x+L,r)=-2\int_0^L\left(\frac{\partial^2}{\partial r^2}v_x\right)_{r=0}dx \tag{41}$$

Once the velocity field for a particular channel geometry and pressure profile is known, the Langevin equation [Eq. (33)] can be solved numerically.

Particle separation across a microchannel is a process of great technological importance.[7,21] Any inhomogeneity in the spatial distribution of an ensemble of non-interacting suspended particles can only be caused by the hydrodynamic interaction between particles and walls.[39] The no-flux boundary condition [Eq. (8)] for unbiased particles with $\vec{F}_{ext}=\vec{0}$ is given by Equation (42):

$$\vec{n}(\vec{x})\cdot\left[\vec{v}(\vec{x})P(\vec{x},t)-\frac{k_BT}{\gamma}\vec{\nabla}P(\vec{x},t)\right]=0\quad\vec{x}\in\text{wall} \tag{42}$$

In the case of vanishing drift velocity normal to the channel walls, $\vec{n}(\vec{x})\cdot\vec{v}(\vec{x})=0$, only uniform distributions are allowed and no particle separation could ever be achieved.[39] However, as anticipated in Section 2.2, for finite-size particles the no-flux boundary condition [Eq. (42)] strictly holds on an effective inner surface at a distance from the channel walls. Due to its finite size, a particle cannot move steadily along a given flow streamline as this gets too close to the walls. Upon hitting the wall, the particle bounces into inner flow streamlines as if they were subject to a transverse field gradient. These hydrodynamic forces may, indeed, lead to accumulation and depletion zones within the channel.

By implementing such a boundary effect, Kettner et al.[59] predicted by numerical simulation that a micron-sized channel with broken reflection symmetry can be used to separate particles according to their size, as illustrated in Figure 5. A time-oscillating pressure profile, $\vec{p}(\vec{x},t)=\vec{p}(\vec{x})f(t)$, where $f(t)$ is a sinusoidal function with frequency ν, is assumed to control the periodic flow of the fluid, back and forth along an infinitely long channel. Within the creeping flow approximation, the ensuing time-dependent velocity field $\vec{v}(\vec{x},t)=\vec{v}(\vec{x})f(t)$ is then obtained in terms of the solution $\vec{v}(\vec{x})$ of the *unperturbed* Stokes equation [Eq. (34)], and the corresponding Langevin equation [Eq. (33)] numerically integrated. Later on, this mechanism was demonstrated experimentally by Matthias and Müller.[60]

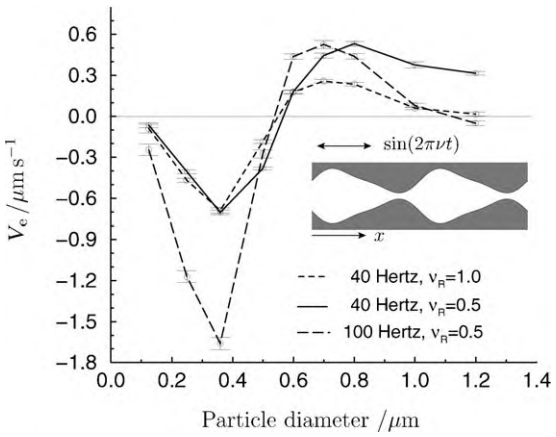

Figure 5. Theoretically evaluated average induced particle current v_e vs particle diameter. The particle is immersed in a laminar flow confined to a channel with broken reflection symmetry (inset). The length of an individual pore is 6 μm with a maximal pore width of 4 μm and a minimal pore width of 1.6 μm. The fluid, with viscosity $\nu_R \equiv \eta/\eta_{water}$ and $\eta_{water} = 1.025 \times 10^3 \mathrm{N\,s\,m^{-2}}$, is periodically pumped back and forth with frequency ν along the x axis of the channel. For further details, see ref. [59].

6. Single-File Diffusion

As the design and the operation of biology-inspired nanodevices[21] have become experimentally affordable, understanding particle diffusion in a 1D potential has been recognized as a key issue in transport control.[27] In this context the particle–particle and particle–wall interactions play a central role. Pair interaction between thermally diffusing particles does not affect the normal character of Brownian diffusion, as long as the particles are able to pass one another, no matter how closely they are confined. This holds true even when, under appropriate temperature and density conditions, attracting particles cluster or condense in the potential wells.[61]

Things change dramatically for strictly 1D geometries. Let us consider, for instance, an ensemble of N unit-mass particles moving with preassigned dynamics along a segment of length l. If the interparticle interaction is hard-core (with zero radius), the elastic collisions between neighboring particles are nonpassing—meaning that the particles can be labeled according to a fixed ordered sequence. The particles are thus arranged into a file where, at variance with the situation described in Section 2, their diffusion is suppressed by the presence of two nonpassing neighbors, also movable in the longitudinal direction.

The diffusion of a free single file (SF), that is, in the absence of a substrate, has been investigated in detail.[33] In the ther-

modynamic limit ($l,N\to\infty$ with constant density $\rho\equiv N/l$) the mean square displacement of each file particle can be written as Equation (43):

$$\langle \Delta x^2(t)\rangle = |\Delta x(t)|/\rho \tag{43}$$

with $|\Delta x(t)|$ denoting the absolute mean displacement of a free particle. For a *ballistic* single file (bSF), clearly $|\Delta x(t)| = \langle |v| \rangle t$, where $\langle \ldots \rangle$ is the ensemble average taken over the distribution of the initial velocities, and therefore Equation (44) follows:

$$\langle \Delta x^2(t)\rangle = \langle |v| \rangle t/\rho \tag{44}$$

A bSF particle apparently diffuses like a Brownian particle with a normal diffusion coefficient $D_0 = \langle |v| \rangle/(2\rho)$. For a *stochastic* single file (sSF) of Brownian particles with damping constant γ at temperature T, the equality $|\Delta x(t)| = \sqrt{4D_0 t/\pi}$ yields the *anomalous* diffusion law of Equation (45):

$$\langle \Delta x^2(t)\rangle = 2D_{SF}\sqrt{t}/\rho \tag{45}$$

where the mobility factor $D_{SF} = \sqrt{D_0/\pi}$ is related to the single-particle diffusion constant $D_0 = k_B T/\gamma$. The onset of the subdiffusive regime of Equation (45) occurs for $t > \tau_d, \tau_d = (D_0\rho^2)^{-1}$, τ_d being the average time a single particle takes to diffuse against one of its neighbors.[62,63] The diffusive regimes [Eqs. (44) and (45)] have been demonstrated both numerically[64] and experimentally.[36,65]

Let $x(t)$ represent the coordinate of one file particle, assumed to be a continuous differentiable stochastic process with $\langle \dot{x}(t)\rangle = 0$. Kubo's relation, Equation (46):[66]

$$\frac{1}{2}\frac{d}{dt}\langle \Delta x^2(t)\rangle = \int_0^t C(\tau)d\tau \quad (t\to\infty) \tag{46}$$

with $C(t)\equiv\langle \dot{x}(t)\dot{x}(0)\rangle$, best illustrates the role of the dimensional constraint on SF diffusion. In the case of normal diffusion, $\langle \Delta x^2(t)\rangle = 2D_0 t$ and the right-hand side of Equation (46) converges to the positive value $D_0 = \int_0^\infty C(\tau)d\tau$. Thus, $x(t)$ diffuses subject to Einstein's law. The subdiffusive dynamics [Eq. (45)] is instead characterized by $\int_0^\infty C(\tau)d\tau = 0$, which, in view of Equation (46), implies that $C(t)$ develops a negative power-law tail $C(t) \sim -c_\beta t^{-\beta}$ with $\beta = \frac{3}{2}$ and $c_\beta = D_{SF}/4\rho$. Numerical simulations support this conclusion. In Figure 6 we report a few curves $C(t)$ for different ρ and γ. The negative tails are apparent and compare well with the estimate derived from Equation (46) [Figure 6, inset]. They are a typical signature of the collisional dynamics in a SF. As an effect of pair collisions, an initial velocity $\dot{x}(0)$ is likely to be compensated by a backflow velocity of opposite sign.[63,67]

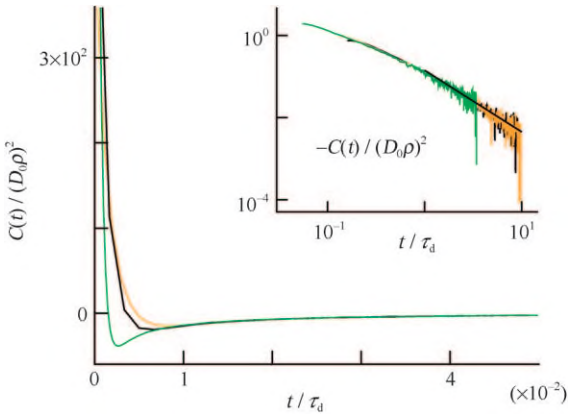

Figure 6. Velocity autocorrelation function $C(t)$ in a sSF at $k_BT = 1$ and for $(\rho,\gamma) = (0.1,3)$ [top, ——], (0.1,5) [middle, ——], and (0.05,5) [bottom, ——]. Inset: log–log plot of the negative $C(t)$ tails; —— is the predicted tail $-D(t)/(D_0\rho)^2 \cong (t/\tau_d)^{-\frac{3}{2}}/(4\sqrt{\pi})$.

6.1. Stochastic Single File on a Substrate

We now focus on the case of a SF diffusing on a sinusoidal substrate with a potential given by Equation (47):[68,69]

$$V(x) = d[1-\cos(2\pi x/L)] \tag{47}$$

This variation of the SF model rises naturally in connection with quasi-1D situations where the particles (not necessarily suspended in a fluid) can be represented by disks moving along a narrow spatially modulated channel with cross-section smaller than twice the disk diameter (see Figure 1 c). The confining action of the channel can be accounted for by modeling the SF dynamics in terms of a periodic substrate potential with an effective strength d. This is the case, for instance, of most nanotubes and zeolite pores.[2]

In the simulations of refs. [63,69] the ith particle was assigned as follows: 1) The particle was given a random initial position, $x_i(0)$, and velocity, $\dot{x}_i(0)$. Upon each elastic collision it switched velocity with either neighbor without altering the file labeling. 2) Independent Brownian dynamics was determined by a viscous force $-\gamma\dot{x}_i$ and a thermal force $\sqrt{2\gamma k_B T}\xi_i(t)$, with $\xi_i(t)$-uncorrelated standard Gaussian noises defined as in Section 2.1, in order to guarantee thermalization at temperature T.

Numerical evidence led to conclude that the periodic substrate potential $V(x)$ does not invalidate the sSF diffusion law of Equation (45), although the dependence of the mobility factor D_{SF} on the system parameters becomes more complicated. In Figures 7 a and b D_{SF} is characterized as a function of γ and T, respectively. The identity $D_{SF} = \sqrt{D_0/\gamma}$, reported above for $V(x)\equiv 0$, applies here, too, under the condition of replacing D_0 with the modified diffusion constant $D(F)$ of Equation (19). In Figure 7 a the rescaled curves $\gamma^{1/2}\langle \Delta x^2(t)\rangle$ versus t overlap asymptotically for any damping regime.

The temperature dependence of the mobility $D_{SF} = \sqrt{D(F)/\gamma}$, is more interesting. As implicit in the discussion of Section 3, this prediction gets more and more accurate for large γ and increasingly high activation-to-thermal energy ratios d/k_BT. As a consequence, the rescaled mobility $\sqrt{\gamma/d}D_{SF}$ turns out to be a function of d/k_BT, alone, in good agreement with the simulation results displayed in Figure 7 c.

6.2. Driven Single Files

Finally, we consider the case of a *driven* sSF, namely, we now assume that all file particles are subjected to an additional con-

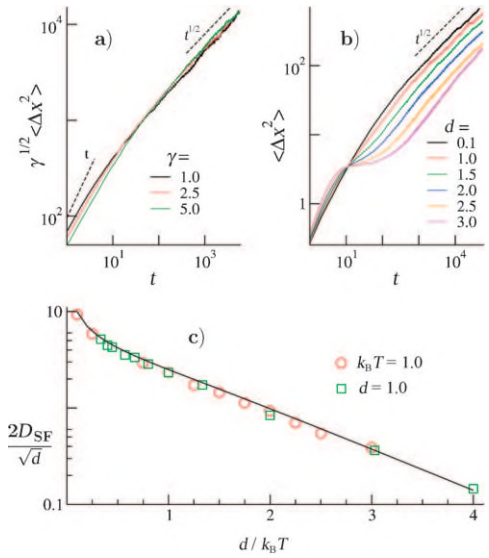

Figure 7. Diffusion of a stochastic single file in the periodic potential of Equation (47)]:[69] a) $\langle \Delta x^2(t) \rangle$ vs t for $k_BT = 1$, $d = 1$ and increasing γ (from top to bottom on the l.h.s), b) $\langle \Delta x^2(t) \rangle$ vs t for $\gamma = 5$ and increasing d (from top to bottom on the r.h.s.). The t and $t^{1/2}$ slopes (-----) have been drawn for the reader's convenience. c) the diffusion mobility D_{SF} vs d/k_BT for $\gamma = 5$ and $d = 1$ (○) and $k_BT = 1$ (□). Other simulation parameters are: $N = 3 \times 10^3, L = 2\pi, l = 3 \times 10^3 L$, and all particles have unit mass.

stant force F pointing, say, to the right ($F \geq 0$). We know from Section 3 that the diffusion of a single Brownian particle drifting down a tilted washboard potential exhibits enhanced normal diffusion with the diffusion constant given by Equation (19). Extensive simulations of a driven SF[69] yielded the numerical data reported in Figure 8. The kinetic mobility of the file, defined as $\mu = \langle \dot{x} \rangle / F$, turns out to coincide with the mobility of a single particle under the same dynamical conditions, irrespective of γ (inset of Figure 8). More remarkably, the subdiffusive regime [Eq. (45)] also applies in the presence of bias,

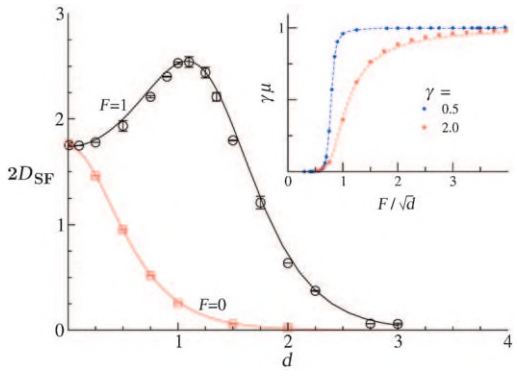

Figure 8. Diffusion of a driven stochastic single file in the periodic potential of Equation (47): the mobility factor D_{SF} vs d for $k_BT = 0.3$, $\gamma = 5$, and $F = 0$ (□) and $F = 1$ (○). (——) represent the law $D_{SF} = \sqrt{D(F)/\pi}$ with $D(F)$ given in Equation (19). Other simulation details are as for Figure 7. Inset: the kinetic mobility, $\mu = \langle \dot{x} \rangle / F$ vs $F/\sqrt{d}$ for $\gamma = 0.5$ (○) and $\gamma = 2$ (□) at $k_BT = 0.1$. The fitting curves are the analytical predictions for a single Brownian particle based, respectively, on Equations (11.194) [low γ] and (11.50) [high γ] of ref. [38].

though with an F-dependent mobility factor. When plotted versus d, D_{SF} attains a maximum enhancement for $d \geq FL/2\pi$, that is, in coincidence with the (noise-assisted) depinning of the file from its sinusoidal substrate. Again, the identity $D_{SF} = \sqrt{D(F)/\pi}$ combined with Equation (19) for D_0 provides an excellent fit of the simulation data for large γ. Of course, the mobility enhancement at depinning can also be revealed by plotting D_{SF} versus F at constant d.

7. Conclusions and Outlook

Herein, we presented the state-of-the-art in diffusive transport in systems characterized by confinement due either to their finite size or to particle interactions in restricted geometries. Confinement plays a salient role in the Brownian motion of driven particles. Indeed, the entropic effects associated with confinement may give rise to anomalous transport features. Some main new phenomena are the entropy-driven decrease of mobility with increasing temperature, the diffusion excess above the free-diffusion limit and the resonant behavior of the effective diffusion coefficient as a function of control parameters such as temperature, external gradients, or geometry design.

The reviewed transport features can thus be implemented in the design of new transport control setups or protocols. In particular, Brownian transport through confined geometries is expected to find application in nanotechnology—for instance, to operate devices for the separation of nanoparticles, to speed up schemes for catalysis on templates, or to realize efficient, driven through-flows of microsized agents, or reactants, in miniaturized lab-on-a-chip devices.

Acknowledgements

This work was made possible thanks to the financial support by: the Volkswagen Foundation (project I/80424, P.H.); the Deutsche Forschungsgemeinschaft (DFG) via projects nos. 1517/26-1 (P.S.B., P.H.), 1517/25-2 (P.H., P.T.) and via the research center, SFB-486, projects A10 and B13 (G.S., P.H., P.T.); the German Excellence Initiative, via the Nanosystems Initiative Munich (NIM) (P.S.B., P.H.); and the Alexander von Humboldt Stiftung, via a Research Award (F.M.).

Keywords: Brownian motion · diffusion · entropy · single-file diffusion · transport

[1] B. Alberts, A. Johnson, J. Lewis, M. Raff, K. Roberts, P. Walter, *Molecular Biology of the Cell*, Garland, New York, **2007**.
[2] J. Kärger, D. M. Ruthven, *Diffusion in Zeolites and Other Microporous Solids*, Wiley, New York, **1992**.
[3] M. C. Daniel, D. Astruc, *Chem. Rev.* **2004**, *104*, 293–346.
[4] A. Corma, *Chem. Rev.* **1997**, *97*, 2373–2419.
[5] R. M. Mazo, *Brownian Motion: Fluctuations, Dynamics and Applications*, Clarendron, Oxford, **2002**.
[6] P. Hänggi, F. Marchesoni, *Chaos* **2005**, *15*, 026101.
[7] P. Hänggi, F. Marchesoni, *arXiv: 0807/1283*.
[8] A. Einstein, *Ann. Phys.* **1905**, *322*, 549–560.
[9] L. Liu, P. Li, S. A. Asher, *Nature* **1999**, *397*, 141–144.

[10] Z. Siwy, I. D. Kosinska, A. Fulinski, C. R. Martin, *Phys. Rev. Lett.* **2005**, *94*, 048102.
[11] Z. Siwy, A. Fulinski, *Am. J. Phys.* **2004**, *72*, 567–574.
[12] K. Healy, *Nanomedicine* **2007**, *2*, 459–481.
[13] K. Healy, B. Schiedt, A. P. Morrison, *Nanomedicine* **2007**, *2*, 875–897.
[14] A. M. Berezhkovskii, M. A. Pustovoit, S. M. Bezrukov, *J. Chem. Phys.* **2007**, *126*, 134706.
[15] I. D. Kosińska, I. Goychuk, M. Kostur, G. Schmid, P. Hänggi, *Phys. Rev. E* **2008**, *77*, 031131.
[16] A. M. Berezhkovskii, S. M. Bezrukov, *Biophys. J.* **2005**, *88*, L17–L19.
[17] A. M. Berezhkovskii, S. M. Bezrukov, *Phys. Rev. Lett.* **2008**, *100*, 038104.
[18] W. Nonner, B. Eisenberg, *J. Mol. Liquids* **2000**, *87*, 149–162.
[19] D. Gillespie, W. Nonner, R. S. Eisenberg, *J. Phys. Condens. Matter* **2002**, *14*, 12129–12145.
[20] D. Boda, D. D. Busath, B. Eisenberg, D. Henderson, W. Nonner, *Phys. Chem. Chem. Phys* **2002**, *4*, 5154–5160.
[21] P. Hänggi, F. Marchesoni, F. Nori, *Ann. Phys.* **2005**, *14*, 51–70.
[22] R. D. Astumian, P. Hänggi, *Phys. Today* **2002**, *55*, 33–39.
[23] P. Reimann, P. Hänggi, *Appl. Phys. A* **2002**, *75*, 169–178.
[24] E. R. Kay, D. A. Leigh, F. Zerbetto, *Angew. Chem.* **2007**, *119*, 72–196; *Angew. Chem. Int. Ed.* **2007**, *46*, 72–191.
[25] V. Balzani, A. Credi, M. Venturi, *ChemPhysChem* **2008**, *9*, 202–220.
[26] a) I. Derényi, R. D. Astumian, *Phys. Rev. E* **1998**, *58*, 7781–7784; b) T. A. J. Duke, R. H. Austin, *Phys. Rev. Lett.* **1998**, *80*, 1552–1555; c) A. Van Oudenaarden, S. G. Boxer, *Science* **1999**, *285*, 1046–1048; d) M. Kostur, L. Schimansky-Geier, *Phys. Lett.* **2000**, *265*, 337–345; e) C. Keller, F. Marquardt, C. Bruder, *Phys. Rev. E* **2002**, *65*, 041927.
[27] L. Machura, M. Kostur, P. Talkner, J. Luczka, F. Marchesoni, P. Hänggi, *Phys. Rev. E* **2004**, *70*, 061105.
[28] a) R. Eichhorn, P. Reimann, P. Hänggi, *Phys. Rev. Lett.* **2002**, *88*, 190601; b) R. Eichhorn, P. Reimann, P. Hänggi, *Phys. Rev. E* **2002**, *66*, 066132; c) L. Machura, M. Kostur, P. Talkner, J. Luczka, P. Hänggi, *Phys. Rev. Lett.* **2007**, *98*, 040601; d) M. Kostur, L. Machura, P. Talkner, P. Hänggi, J. Luczka, *Phys. Rev. B* **2008**, *77*, 104509.
[29] a) J. Currie, J. A. Krumhansl, A. R. Bishop, S. E. Trullinger, *Phys. Rev. B* **1980**, *22*, 477–496; b) G. Costantini, F. Marchesoni, *Phys. Rev. Lett.* **2001**, *87*, 114102.
[30] E. Arvanitidou, D. Hoagland, *Phys. Rev. Lett.* **1991**, *67*, 1464–1466.
[31] J. J. Kasianowicz, E. Bradin, D. Branton, D. W. Deemer, *Proc. Natl. Acad. Sci. USA* **1996**, *93*, 13770–13773.
[32] a) J. Han, S. W. Turner, H. G. Craighead, *Phys. Rev. Lett.* **1999**, *83*, 1688–1691; b) J. Han, H. G. Craighead, *Science* **2000**, *288*, 1026–1029.
[33] a) D. W. Jepsen, *J. Math. Phys.* **1965**, *6*, 405–413; b) D. G. Levitt, *Phys. Rev. A* **1973**, *8*, 3050–3054; c) T. E. Harris, *Ann. Probab.* **1974**, *2*, 969–988; d) J. K. Percus, *Phys. Rev. A* **1974**, *9*, 557–559.
[34] a) H. Lamb, *Hydrodynamics*, Dover, New York, **1945**; b) L. G. Leal, *Laminar Flow and Convective Transport*, Butterworth–Heinmann, Boston, **1992**; c) Z. U. A. Warsi, *Fluid Dynamics*, CRC, Boca Raton, **1992**.
[35] B. Cui, H. Diamant, B. Lin, *Phys. Rev. Lett.* **2002**, *89*, 188302.
[36] Q. H. Wei, C. Bechinger, P. Leiderer, *Science* **2000**, *287*, 625–627.
[37] E. M. Purcell, *Am. J. Phys.* **1977**, *45*, 3–11.
[38] H. Risken, *The Fokker–Planck Equation, 2nd ed.*, Springer, Berlin, **1989**.
[39] M. Schindler, P. Talkner, P. Hänggi, *Physica A* **2007**, *385*, 46.
[40] S. M. Bezrukov, A. M. Berezhkovskii, M. A. Pustovoit, A. Szabo, *J. Chem. Phys.* **2000**, *113*, 8206–8211.
[41] M. S. Dresselhaus, G. Dresselhaus, P. C. Eklund, *The Science of Fullerenes and Carbon Nanotubes*, Academic Press, New York, **1996**.
[42] P. Hänggi, P. Talkner, *Phys. Rev. A* **1985**, *32*, 1934–1937.
[43] P. Hänggi, P. Talkner, M. Borkovec, *Rev. Mod. Phys.* **1990**, *62*, 251–342.
[44] a) P. Reimann, C. Van den Broeck, H. Linke, P. Hänggi, J. M. Rubí, A. Pérez-Madrid, *Phys. Rev. Lett.* **2001**, *87*, 010602; b) P. Reimann, C. Van den Broeck, H. Linke, P. Hänggi, J. M. Rubi, A. Perez-Madrid, *Phys. Rev. E* **2002**, *65*, 031104.
[45] R. L. Stratonovich, *Radiotekhnika i elektronika* **1958**, *3*, 497–511.
[46] V. I. Tikhonov, *Avtom. Telemekh.* **1959**, *20*, 1188–1196.
[47] S. Lifson, J. L. Jackson, *J. Chem. Phys.* **1962**, *36*, 2410–2414.
[48] G. Costantini, F. Marchesoni, *Europhys. Lett.* **1999**, *48*, 491–497.
[49] C. Cattuto, G. Costantini, T. Guidi, F. Marchesoni, *Phys. Rev. B* **2001**, *63*, 094308.
[50] a) I. Goychuk, E. Heinsalu, M. Patriarca, G. Schmid, P. Hänggi, *Phys. Rev. E* **2006**, *73*, 020101(R); b) E. Heinsalu, M. Patriarca, I. Goychuk, P. Hänggi, *J. Phys. Condens. Matter* **2007**, *19*, 065114.
[51] M. H. Jacobs, *Diffusion Processes*, Springer, New York, **1967**.
[52] R. Zwanzig, *J. Phys. Chem.* **1992**, *96*, 3926–3930.
[53] D. Reguera, J. M. Rubí, *Phys. Rev. E* **2001**, *64*, 061106.
[54] P. Kalinay, J. K. Percus, *Phys. Rev. E* **2006**, *74*, 041203.
[55] P. S. Burada, G. Schmid, D. Reguera, J. M. Rubí, P. Hänggi, *Phys. Rev. E* **2007**, *75*, 051111.
[56] D. Reguera, G. Schmid, P. S. Burada, J. M. Rubí, P. Reimann, P. Hänggi, *Phys. Rev. Lett.* **2006**, *96*, 130603.
[57] N. Laachi, M. Kenward, E. Yariv, K. D. Dorfman, *Europhys. Lett.* **2007**, *80*, 50009.
[58] P. S. Burada, G. Schmid, P. Talkner, P. Hänggi, D. Reguera, J. M. Rubí, *BioSystems* **2008**, *93*, 16–22.
[59] C. Kettner, P. Reimann, P. Hänggi, F. Müller, *Phys. Rev. E* **2000**, *61*, 312–323.
[60] a) S. Matthias, F. Müller, *Nature* **2003**, *424*, 53–57; b) F. Müller, A. Birner, J. Schilling, U. Gösele, C. Kettner, P. Hänggi, *Phys. Status Solidi A* **2000**, *182*, 585–590.
[61] a) S. Savel'ev, F. Marchesoni, F. Nori, *Phys. Rev. Lett.* **2003**, *91*, 010601; b) S. Savel'ev, F. Marchesoni, F. Nori, *Phys. Rev. Lett.* **2004**, *92*, 160602.
[62] K. K. Mon, J. K. Percus, *J. Chem. Phys.* **2002**, *117*, 2289–2292.
[63] F. Marchesoni, A. Taloni, *Phys. Rev. Lett.* **2006**, *97*, 106101.
[64] a) P. M. Richards, *Phys. Rev. B* **1977**, *16*, 1393–1409; b) H. Van Beijeren, K. W. Kehr, R. Kutner, *Phys. Rev. B* **1983**, *28*, 5711–5723; c) J. Kärger, M. Petzold, H. Pfeifer, S. Ernst, J. Weitkamp, *J. Catal.* **1992**, *136*, 283–299; d) D. S. Sholl, K. A. Fichthorn, *Phys. Rev. E* **1997**, *55*, 7753–7756.
[65] a) P. Demontis, G. B. Suffritti, S. Quartieri, E. S. Fois, A. Gamba, *J. Phys. Chem.* **1988**, *92*, 867–871; b) R. L. June, A. T. Bell, D. N. Theodorou, *J. Phys. Chem.* **1990**, *94*, 8232–8240; c) K. Hahn, J. Kärger, V. Kukla, *Phys. Rev. Lett.* **1996**, *76*, 2762–2765.
[66] R. Kubo, *Rep. Prog. Phys.* **1966**, *29*, 255–284.
[67] F. Marchesoni, A. Taloni, *Chaos* **2007**, *17*, 043112.
[68] J. K. Percus, *J. Stat. Phys.* **1976**, *15*, 505–511.
[69] a) A. Taloni, F. Marchesoni, *Phys. Rev. Lett.* **2006**, *96*, 020601; b) A. Taloni, F. Marchesoni, *Phys. Rev. E* **2006**, *74*, 051119.